

Temperature-Controlled Release of Diols from *N*-Isopropylacrylamide-*co*-Acrylamidophenylboronic Acid Microgels

Hui Ge, Yanwei Ding, Chengcheng Ma, and Guangzhao Zhang*

Hefei National Laboratory for Physical Sciences at Microscale, Department of Chemical Physics, University of Science and Technology of China, Hefei, Anhui, China

Received: February 13, 2006; In Final Form: May 13, 2006

N-Isopropylacrylamide-*co*-acrylamidophenylboronic acid (NIPAM-*co*-PBA) microgels were prepared by free radical polymerization in water. The release of glucose and Alizarin Red S (ARS) from the microgels as a function of temperature has been investigated by using laser light scattering (LLS) and ultrasensitive differential scanning calorimetry (US-DSC). Such microgels can bind glucose and ARS via boronic acids at a lower temperature. As the temperature increases, the microgels shrink, and the diols are released. The release could be controlled by temperature. The effect of the structure of the microgels on the release is also discussed.

Introduction

Stimuli-responsive polymers which change their behaviors and functions in response to chemical or physical stimuli have received much attention because of their potential use in drug delivery, bioseparation, and biocatalysts.^{1,2} It is known that boronic acid can bind diols through reversible boronate ester formation;^{3,4} i.e., it exhibits a diol sensitivity. Boronic acid carrying polymers have been used in the recognition, detection, isolation, and transport of diol compounds such as carbohydrates, vitamins, coenzymes, and ribonucleic acids (RNAs).^{5–23} Particularly, such a polymer is potentially developed into a self-regulating insulin delivery system for the treatment of diabetes.^{24,25} Since poly(*N*-isopropylacrylamide) (PNIPAM) is a well-known thermoresponsive polymer with a lower critical solution temperature (LCST) around ~32 °C,²⁶ *N*-isopropylacrylamide-*co*-acrylamidophenylboronic acid (NIPAM-*co*-PBA) copolymers demonstrate both temperature and diol responses. Actually, linear copolymers,^{16–19} gels,²¹ and latex^{21,22} of NIPAM-*co*-PBA have been prepared in organic solvents and water, and their responsive behaviors were also investigated. However, the roles that temperature and structure of the copolymers played in absorption and release are not clear yet.

In the present work, we prepared NIPAM-*co*-PBA microgels via free radical polymerization in water at a temperature above the LCST of PNIPAM. Using laser light scattering (LLS) and ultrasensitive differential scanning calorimetry (US-DSC), we have investigated the release of Alizarin Red S and glucose from the microgels as a function of temperature.

Experiment Section

Materials. *N*-Isopropylacrylamide (NIPAM) from Aldrich was recrystallized three times from an *n*-hexane/acetone mixture prior to use. *N,N*-Methylenebisacrylamide (BIS) from Sinopharm was purified by recrystallization from methanol. Potassium persulfate (KPS) from Sinopharm was recrystallized from deionized water. The details about the synthesis of 3-(arylamido)phenylboronic acid (PBA) can be found elsewhere.^{6,27} Alizarin Red S (ARS), glucose, sodium dodecyl sulfate (SDS),

and sodium hydroxide were all from Sinopharm and used without further purification.

Microgel Preparation. The preparation of the microgel is detailed elsewhere.²⁸ Typically, NIPAM (0.501 g), PBA (0.083 g), SDS (0.023 g), and BIS (0.015 g) were dissolved in deionized water (40 mL) in a 100 mL three-necked flask. After the reactor was purged with bubbling nitrogen for 30 min, 0.0162 g of KPS in 10 mL of deionized water was introduced. The mixture was stirred under nitrogen bubbling at 70 °C for 8 h. The resulting solution was dialyzed for 1 week against deionized water using a semipermeable membrane with a molar mass cutoff of 10⁴ g/mol to remove the unreacted monomers and SDS.

Bulk gel was prepared in 1,4-dioxane (40 mL) with the same feed of NIPAM, PBA, and BIS under nitrogen bubbling at 70 °C for 8 h. After the resulting gel was crushed, about 40 mL of water was introduced to precipitate the gel. Thus, most of the 1,4-dioxane and the unreacted monomers were removed. Such a microgel (NIPAM-*ran*-PBA) was further micronized using a commercial whisk machine. To get rid of the trace amount of dioxane and the unreacted monomers, the resulting solution was dialyzed for 1 week against deionized water using a semipermeable membrane with a molar mass cutoff of 10⁴ g/mol. The microgel solution was filtrated with a 0.45 μm filter so that NIPAM-*ran*-PBA microgels with an average hydrodynamic radius of ~70 nm at 25 °C were obtained. In parallel, a linear NIPAM-*ran*-PBA copolymer was synthesized with the same amount of NIPAM and PBA in 1,4-dioxane under the same conditions. NIPAM and PBA in the microgels and linear chains prepared in 1,4-dioxane are expected to be randomly distributed since 1,4-dioxane is a good solvent for both PNIPAM and poly-(acrylamidophenylboronic acid) (PPBA).

The content of phenylboronate was determined by ¹H NMR on a Bruker DMX-300 NMR spectrometer with DMSO-*d*₆ as the solvent and tetramethylsilane (TMS) as the internal standard. The NIPAM-*co*-PBA microgels prepared in water have 18 mol % PBA. The PBA contents of linear NIPAM-*ran*-PBA copolymer and microgels prepared in dioxane are 17 and 16 mol %, respectively.

Photography. The microgel solutions with ARS at pH 10 as a function of temperature were photographed by use of a 5 megapixel camera (Canon Powershot A95). The concentrations

* To whom correspondence should be addressed.

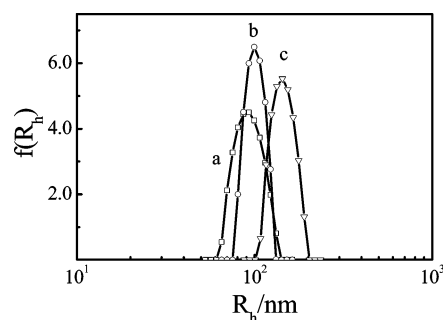


Figure 1. Hydrodynamic radius distributions $f(R_h)$ of NIPAM-*co*-PBA microgels in aqueous solution at 20 °C with pH 6.5 (a), 9.2 (b), and 10.0 (c), where the concentration of the microgels is 1×10^{-5} g/mL.

of the microgel and ARS were 2.0×10^{-3} and 1.0×10^{-4} g/mL, respectively. The pH of a microgel solution was adjusted by adding a certain amount of NaOH aqueous solution.

Ultrasensitive Differential Scanning Calorimetry (US-DSC). US-DSC measurements were performed on a VP-DSC calorimeter from MicroCal. A dilute NaOH solution with pH 10.0 was used as the reference. The polymer solutions were degassed at 25 °C for 1/2 h and then equilibrated at 10 °C for 2 h before the measurements. The concentration of the microgel solutions was 2.0×10^{-3} g/mL, and the concentrations of glucose and ARS were 1.0×10^{-4} g/mL. The heating rate was 1.0 °C/min. The deconvolution analysis was done with a MicroCal Origin Software, which allows the complex endotherm to be resolved into several Gaussian distributions.

Laser Light Scattering (LLS). The LLS measurements were conducted on an ALV/DLS/SLS-5022F spectrometer with a multi- τ digital time correlation (ALV5000) and a cylindrical 22 mW UNIPHASE He–Ne laser ($\lambda_0 = 632$ nm) as the light source. In static LLS,^{29,30} we were able to obtain the weight-average molar mass (M_w), the root-mean-square radius of gyration $\langle R_g^2 \rangle_z^{1/2}$ (or written as $\langle R_g \rangle$), and the second virial coefficient A_2 from the angular dependence of the absolute excess time-average scattering intensity, known as the Rayleigh ratio $R_{vv}(q)$. In dynamic LLS,³¹ the intensity–intensity time correlation function $G^{(2)}(t, q)$ was measured to determine the line width distribution $G(\Gamma)$. For diffusive relaxation, Γ is related to the translational diffusion coefficient (D) of the scattering object (polymer chain or colloid particle) in dilute solution or dispersion by $D = \langle \Gamma \rangle / q^2$ and further to the hydrodynamic radius (R_h) from the Stokes–Einstein equation $R_h = k_B T / (6\pi\eta D)$, where η , k_B , and T are the solvent viscosity, the Boltzmann constant, and the absolute temperature, respectively. The hydrodynamic radius distribution $f(R_h)$ was calculated from the Laplace inversion of a corresponding measured $G^{(2)}(t, q)$ using the CONTIN program. All the dynamic LLS measurements were conducted at a small scattering angle (θ) of 15°.

Results and Discussion

Figure 1 shows the typical hydrodynamic radius distributions ($f(R_h)$) of NIPAM-*co*-PBA microgels at 20 °C with pH 6.5, 9.2, and 10.0, respectively, where the microgels prepared in water have a concentration (C) of 1.0×10^{-5} g/mL. It shows that the average hydrodynamic radius ($\langle R_h \rangle$) of the microgels increases with pH. This is understandable because the pK_a of PBA in NIPAM-*co*-PBA copolymer is 8.8–9.1.¹⁸ At pH 6.5, 9.2, and 10.0, boronic acid groups are uncharged, partially charged, and completely charged, respectively. A higher pH leads the microgels to be more swollen with a larger size.

Figure 2 shows the temperature dependence of the average hydrodynamic radius ($\langle R_h \rangle$) of NIPAM-*co*-PBA microgels pre-

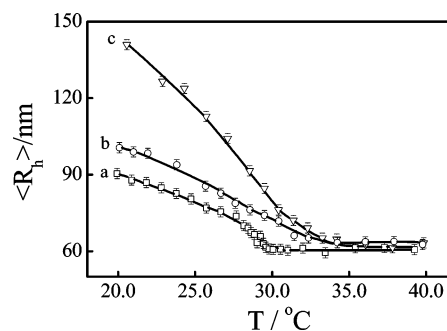


Figure 2. Temperature dependence of average hydrodynamic radius ($\langle R_h \rangle$) of NIPAM-*co*-PBA microgels in aqueous solution at pH 6.5 (a), 9.2 (b), and 10.0 (c), where the concentration of the microgels is 1×10^{-5} g/mL.

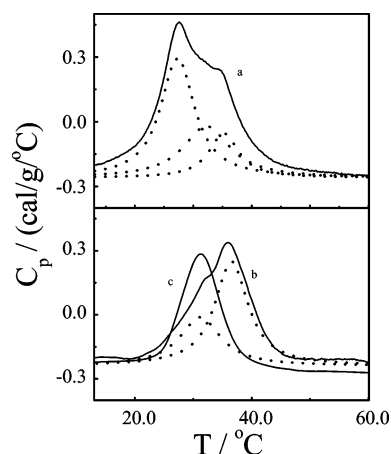


Figure 3. Temperature dependence of specific heat capacity (C_p) of the microgels and linear chains at pH 10.0, where the concentrations are 2×10^{-3} g/mL. (a) NIPAM-*co*-PBA microgels prepared in water; (b) NIPAM-*ran*-PBA microgels prepared in dioxane; (c) linear NIPAM-*ran*-PBA copolymer prepared in dioxane. The solid lines and dotted lines correspond to experimental and deconvoluted data, respectively.

pared in water at pH 6.5, 9.2, and 10.0, respectively. At each pH, $\langle R_h \rangle$ decreases with increasing temperature, indicating the shrinking of the thermoresponsive microgels. The size of the microgels finally tends to be a constant because the microgels stop shrinking at temperatures above their LCSTs. It should be noted that the excess scattering intensity $R_{vv}(\theta)/KC$ did not have a temperature dependence in the range we investigated, indicating that no aggregation occurred, because $R_{vv}(\theta)/KC$ is proportional to the weight-average molar mass (M_w) of the scattering object, and it is very sensitive to aggregation. On the other hand, in contrast to PNIPAM microgels with a sharp phase transition,²⁸ NIPAM-*co*-PBA microgels exhibit a smooth transition depending on pH. This might be because the latter have a less uniform structure.

Figure 3 shows the temperature dependence of the specific heat capacity (C_p) of the solutions of NIPAM-*co*-PBA microgels, NIPAM-*ran*-PBA microgels, and linear NIPAM-*ran*-PBA chains at pH 10.0. NIPAM-*co*-PBA microgels prepared in water exhibit a broad transition which could be deconvoluted into three peaks centered at 27, 31, and 36 °C, respectively. It is known that the preparation conditions have serious effects on the comonomer distribution of the copolymers containing NIPAM units. Previous studies revealed that the polymerization at temperatures below and near the LCST of PNIPAM usually leads to a random copolymer, but the copolymer has a segmented distribution when the polymerization occurs at a temperature above the LCST.^{32–34} In the present study, NIPAM-*co*-PBA microgels were prepared



Figure 4. Photographs of NIPAM-co-PBA microgels in the presence of ARS at different temperatures, where the concentrations of the microgels and ARS are 2×10^{-3} and 1×10^{-4} g/mL, respectively.

at 70 °C, where water is a poor solvent for both PNIPAM and PPBA; the comonomers might be segmentally distributed. In contrast, NIPAM and PBA are expected to randomly copolymerize in 1,4-dioxane because it is a good solvent for both PNIPAM and PPBA.

To clarify the complex transition of NIPAM-co-PBA microgels prepared in water, solutions of linear NIPAM-*ran*-PBA chains and NIPAM-*ran*-PBA microgels prepared in 1,4-dioxane have also been examined. Figure 3 shows that the transition of the linear NIPAM-*ran*-PBA chains has only one peak centered at ~ 31 °C, indicating that the comonomers copolymerize randomly in 1,4-dioxane. NIPAM-*ran*-PBA microgels exhibit a broad transition which could be deconvoluted into two peaks at ~ 31 and ~ 36 °C. Such peaks can be also found in the NIPAM-co-PBA microgels prepared in water. Reasonably, the former should be associated with the collapse of relatively free random NIPAM-co-PBA segments, whereas the latter should be attributed to the collapse of random NIPAM-co-PBA segments in the vicinity of the cross-links, since the restriction leads the LCST of the segments to shift to a higher temperature. Note that PNIPAM microgels show a transition at ~ 32 °C, very close to the former. However, our experiments revealed that the transitions of the NIPAM-co-PBA microgels and linear NIPAM-*ran*-PBA chains have much pH dependence; i.e., each transition shifts to a lower temperature with decreasing pH, but the transition of PNIPAM slightly changes with pH in the range pH 6.5–10.0. Accordingly, the peak at ~ 31 °C could not be attributed to the collapse of PNIPAM segments. On the other hand, a previous study¹⁸ and our experiments show that the random NIPAM-*ran*-PBA copolymer exhibits a LCST at ~ 27 °C at pH 6.5, where the boronic acid groups are uncharged. It is known that PPBA homopolymer is insoluble in an aqueous solution at pH 10; i.e., the boronic acid groups in the homopolymer are still uncharged at pH 10. Thus, the peak at ~ 27 °C for the microgels prepared in water might be attributed to the collapse of segmental NIPAM-co-PBA segments containing many more PBA units. In other words, the microgels prepared in water might have an “island/ocean” structure with PBA-rich domains as the “islands” and PNIPAM segments as the “ocean”. In the following, we will discuss the release of diols from such microgels.

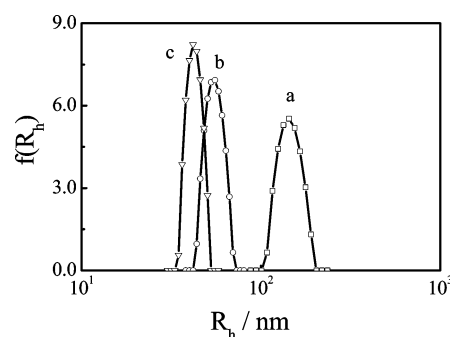


Figure 5. Hydrodynamic radius distributions $f(R_h)$ of NIPAM-co-PBA microgels in the absence (a) and presence of glucose (b) and ARS (c) at 20 °C with pH 10.0, where the concentrations of the microgels, glucose and ARS are 1×10^{-5} , 1×10^{-3} , and 1×10^{-3} g/mL, respectively.

The photographs in Figure 4 show the temperature effect on the release of ARS from NIPAM-co-PBA microgel at pH 10.0, where the molar ratio of PBA to ARS is 3/1. ARS is known to bind phenylboronic acid and shows different colors depending on the conditions.^{35–38} Pure ARS solution is purple at pH 10.0. When it binds with boronic acid, the color turns orange. Figure 4 shows that the microgel solution is orange when it is mixed with ARS at 20 °C, indicating that ARS molecules bind boronic acids or are absorbed by the microgels. As the temperature increased, the color gradually changed from orange to purple. At a temperature above the LCST (~ 31 °C), the color was close to that of ARS solution, suggesting that the ARS molecules no longer bind the boronic acids; namely, ARS molecules in the microgels were squeezed out or released at a high temperature due to the collapse of NIPAM-co-PBA segments. Actually, we found that such temperature-induced color was visible even when the concentration of ARS was as low as 2.0×10^{-6} g/mL. Therefore, the microgels might be used in colorimetric determination.

Figure 5 shows hydrodynamic radius distributions ($f(R_h)$) of NIPAM-co-PBA microgels after the addition of glucose and ARS at 20 °C, where the pH of the microgel solutions was 10.0. The introduction of either glucose or ARS resulted in a decrease in the size of the microgel. This is because the diols form

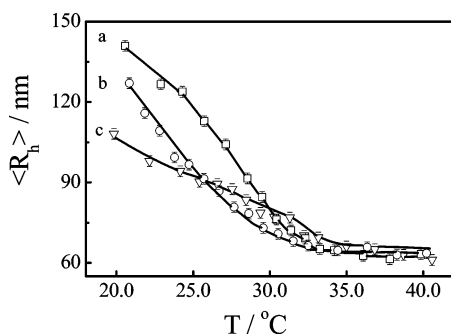


Figure 6. Temperature dependence of average hydrodynamic radius $\langle R_h \rangle$ of NIPAM-co-PBA microgels in the absence (a) and presence of glucose (b) and ARS (c) solution at pH 10.0, where the concentrations of the microgels, glucose, and ARS are 1×10^{-5} , 1×10^{-3} , and 1×10^{-3} g/mL, respectively.

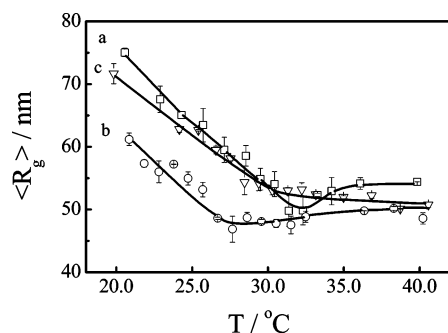


Figure 7. Temperature dependence of average radius of gyration $\langle R_g \rangle$ of NIPAM-co-PBA microgel in the absence (a) and presence of glucose (b) and ARS (c) solution at pH 10.0, where the concentrations of the microgels, glucose, and ARS are 1×10^{-5} , 1×10^{-3} , and 1×10^{-3} g/mL, respectively.

complexes with boronic acid groups and physically cross-link the segments between two chemically cross-linking sites,²³ leading the microgels to shrink. In our preliminary experiments, we found that further increasing the concentration of the glucose or ARS would not change the $\langle R_h \rangle$ of microgels since the amount of diols is enough to bind all boronic acid groups. This indicates that the diols are probably not physically trapped in the microgels. Figure 5 also shows that ARS caused more of a decrease in $\langle R_h \rangle$ than glucose. This might be because the anthraquinone moiety of the ARS molecule binds the hydrophobic moieties of NIPAM-co-PBA segments, and ARS molecules act as a multi-cross-linker, leading the microgel to collapse more. As discussed above, boronic acids in PBA-rich domains are not expected to be charged; the diols should bind the boronic acids in the random NIPAM-co-PBA segments.

Figure 6 shows the temperature dependence of the hydrodynamic radius $\langle R_h \rangle$ of NIPAM-co-PBA microgel at pH 10.0 in the presence of glucose or ARS. The addition of glucose or ARS led the size of microgels to decrease at low temperatures. As the temperature increases, the difference in size between the microgels in the absence and presence of glucose or ARS gradually diminishes. Above ~ 31 °C, there is almost no difference between them, suggesting that either glucose or ARS has been released as the temperature increases up to the LCST of the copolymer.

Figure 7 shows the temperature dependence of the radius of gyration $\langle R_g \rangle$ of NIPAM-co-PBA microgels at pH 10.0 in the presence of glucose or ARS. As expected, $\langle R_g \rangle$ decreased after the microgels were mixed with glucose or ARS at 20 °C, further indicating that the diols bind the boronic acids. Note that glucose led to a larger decrease in $\langle R_g \rangle$ than ARS. This is different from

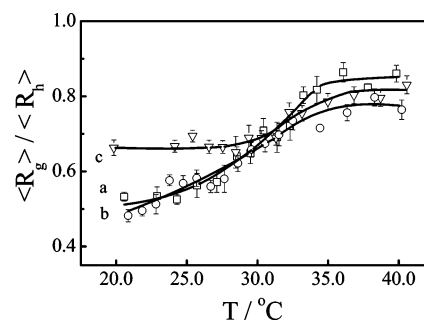


Figure 8. Temperature dependence of $\langle R_g \rangle / \langle R_h \rangle$ of NIPAM-co-PBA microgels in the absence (a) and presence of glucose (b) and ARS (c) solution at pH 10.0, where the concentrations of the microgels, glucose, and ARS are 1×10^{-5} , 1×10^{-3} , and 1×10^{-3} g/mL, respectively.

what happened to $\langle R_h \rangle$. It is known that R_g is related to the distribution of mass according to its definition. Since each glucose molecule has more hydroxyls than an ARS molecule, more ARS molecules are needed to bind all the boronic acids in the microgels; namely, a greater mass of ARS complexed with the microgel, leading to a smaller decrease in $\langle R_g \rangle$. As the temperature increases, $\langle R_g \rangle$ values of the microgels in the presence of glucose and ARS approach that without the diols, implying the release of the diols. However, even at temperatures above the LCST of the copolymer, the $\langle R_g \rangle$ of the microgels with glucose or ARS is somewhat smaller than that without the diols, suggesting a minor amount of diols still inside the microgels at higher temperatures though they have little effect on $\langle R_h \rangle$ as shown in Figure 6.

Figure 8 shows the temperature dependence of the ratio of the average radius of gyration to the average hydrodynamic radius $\langle R_g \rangle / \langle R_h \rangle$ of NIPAM-co-PBA microgels at pH 10.0 in the absence and presence of glucose or ARS. $\langle R_g \rangle / \langle R_h \rangle$ of the microgels increased from ~ 0.5 to ~ 0.8 with increasing temperature. The small $\langle R_g \rangle / \langle R_h \rangle$ value at low temperatures suggests that the microgels are "hairy". As temperature increases, the hairs collapse and the ratio increases. The higher $\langle R_g \rangle / \langle R_h \rangle$ for the microgels in the presence of ARS at temperatures below the LCST suggests that ARS molecules form complexes with the boronic acids both inside the microgels and in the hairs, leading the hairs to shrink. At a temperature above the LCST, there is almost no difference in $\langle R_g \rangle / \langle R_h \rangle$ between the microgels in the absence and presence of diols, implying that the diols have been released.

Figure 9 shows the temperature dependence of the specific heat capacity (C_p) of NIPAM-co-PBA microgel solution in the presence of the diols at pH 10.0. The microgels with glucose demonstrate a bimodal transition with one peak at ~ 36 °C and the other at ~ 31 °C. Meanwhile, the microgel with the absorbed ARS exhibits only one exothermic peak centered at ~ 33 °C. In comparison with the results shown in Figure 3, the peak at ~ 27 °C disappears, indicates that the motion of PBA-rich domains have been depressed by the cross-linking of the glucose or ARS. Furthermore, due to the multi-cross-linking of ARS, ARS can cross-link the NIPAM-co-PBA segments in the microgels more effectively, so that the microgels exhibit a single exothermic transition. In contrast, the glucose molecules could cross-link NIPAM-co-PBA segments much less completely; some segments are still relatively free, leading to a bimodal transition. This agrees with the light scattering results discussed above.

Conclusion

In conclusion, we have prepared *N*-isopropylacrylamide-co-acrylamidophenylboronic acid (NIPAM-co-PBA) microgels in

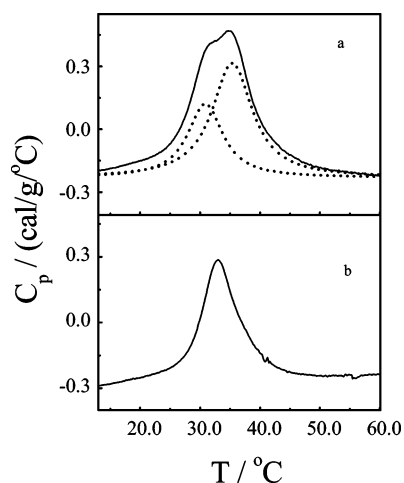


Figure 9. Temperature dependence of C_p of NIPAM-co-PBA microgels in the presence of glucose (a) and ARS (b) at pH 10.0, where the concentrations of the microgels, glucose, and ARS are 1×10^{-5} , 1×10^{-3} , and 1×10^{-3} g/mL, respectively. The solid lines are the experimental data and the dotted lines are deconvoluted data.

water. Using laser light scattering and ultrasensitive differential scanning calorimetry, we have investigated the temperature effects on the release of glucose and ARS from the microgels. The diols can be absorbed by the microgels at a low temperature. As temperature increases up to the LCST of the copolymer, the diols are released due to the shrinking of the microgels. Such a release can be well controlled by temperature. The NIPAM-co-PBA microgels might be used in the temperature-controlled delivery of drugs or biomolecules with diols.

Acknowledgment. The financial support of the National Natural Science Foundation (NNSF) of China (20474060) and The Chinese Academy of Sciences (KJCX2-SW-H14) is gratefully acknowledged.

References and Notes

- Galaev, I. Y.; Mattiasson, B. *Trends Biotechnol.* **1999**, *17*, 335.
- Osada, Y.; Ross-Murphy, S. B. *Sci. Am.* **1993**, *268*, 82.
- Striegler, S. *Curr. Org. Chem.* **2003**, *7*, 81.
- Otsuka, H.; Uchimura, E.; Koshino, H.; Okano, T.; Kataoka, K. *J. Am. Chem. Soc.* **2003**, *125*, 3493.
- Kitano, H.; Kuwayama, M.; Knayama, N.; Ohno, K. *Langmuir* **1998**, *14*, 165.
- Kitano, S.; Koyama, Y.; Kataoka, K.; Okano, T.; Sakurai, Y. *J. Controlled Release* **1992**, *19*, 161.
- Gao, S.; Wang, W.; Wang, B. *Bioorg. Chem.* **2001**, *29*, 308.
- Appleton, B.; Gibson, T. D. *Sens. Actuators, B* **2000**, *65*, 302.
- Westmark, P. R.; Gardiner, S. J.; Smith, B. D. *J. Am. Chem. Soc.* **1996**, *118*, 11093.
- Gabai, R.; Sallacan, N.; Chegel, V.; Bourenko, T.; Katz, E.; Willner, I. *J. Phys. Chem. B* **2001**, *105*, 8196.
- Cannizzo, C.; Amigoni-Gerbier, S.; Larpent, C. *Polymer* **2005**, *46*, 1269.
- Choi, Y. K.; Jeong, S. Y.; Kim, Y. H.; Jeong, S. Y. *Int. J. Pharm.* **1992**, *80*, 9.
- Shiino, D.; Murata, Y.; Kubo, A.; Kim, Y. J.; Kataoka, K.; Koyama, Y.; Kikuchi, A.; Yokoyama, M.; Sakurai, Y.; Okano, T. *J. Controlled Release* **1995**, *37*, 269.
- Uchimura, E.; Otsuka, H.; Okano, T.; Sakurai, Y.; Kataoka, K. *Biotechnol. Bioeng.* **2001**, *72*, 307.
- Niwa, M.; Sawada, T.; Higashi, N. *Langmuir* **1998**, *14*, 3916.
- Kikuchi, A.; Suzuki, K.; Okabayshi, O.; Hoshino, H.; Kataoka, K.; Sakurai, Y.; Okano, T. *Anal. Chem.* **1996**, *68*, 823.
- Matsumoto, A.; Ikeda, S.; Harada, A.; Kataoka, K. *Biomacromolecules* **2003**, *4*, 1410.
- Shimori, K.; Ivanov, A. E.; Galaev, I. Y.; Kawano, Y.; Mattiasson, B. *Macromol. Chem. Phys.* **2004**, *205*, 27.
- Kataoka, K.; Miyazaki, H.; Okano, T.; Sakurai, Y. *Macromolecules* **1994**, *27*, 1061.
- Kataoka, K.; Miyazaki, H.; Bunya, M.; Okano, T.; Sakurai, Y. *J. Am. Chem. Soc.* **1998**, *120*, 12694.
- Elmas, B.; Onur, M. A.; Senel, S.; Tuncel, A. *Colloid Polym. Sci.* **2002**, *280*, 1137.
- Elmas, B.; Onur, M. A.; Senel, S.; Tuncel, A. *Colloid. Surf., A* **2004**, *232*, 253.
- Vladimir, L. A.; Anjal, C. S.; Alexander, V. G.; Sasmita, D.; Igor, K. L.; Graig, S. W.; David, N. F.; Sanford, A. A. *Anal. Chem.* **2003**, *75*, 2316.
- Jeong, S. Y.; Kim, S. W.; Eenink, M. J. D.; Feijen, J. *J. Controlled Release* **1984**, *1*, 57.
- Sato, S.; Jeong, S. Y.; McRea, J. C.; Kim, S. W. *J. Controlled Release* **1984**, *1*, 67.
- Schild, H. G. *Prog. Polym. Sci.* **1992**, *17*, 163.
- William, S.; John, R. J. *J. Am. Chem. Soc.* **1931**, *53*, 711.
- Zhao, Y.; Zhang, G. Z.; Wu, C. *Macromolecules* **2001**, *34*, 7804.
- Zimm, B. H. *J. Chem. Phys.* **1948**, *16*, 1099.
- Chu, B. *Laser Light Scattering*, 2nd ed.; Academic Press: New York, 1991.
- Berne, B.; Pecora, R. *Dynamic Light Scattering*; Plenum Press: New York, 1976.
- Virtanen, J.; Baron, C.; Tenhu, H. *Macromolecules* **2000**, *33*, 336.
- Lozinsky, V. I.; Simenel, I. A.; Kulakova, V. K.; Kurskaya, E. A.; Babushkina, T. A.; Klimova, T. P.; Burova, T. V.; Dubovik, A. S.; Grinberg, V. Y.; Galaev, I. Y.; Mattiasson, B.; Khokhlov, A. R. *Macromolecules* **2003**, *36*, 7308.
- Siu, M. H.; He, C.; Wu, C. *Macromolecules* **2003**, *36*, 6588.
- Arimori, S.; Ward, C. J.; James, T. D. *Tetrahedron Lett.* **2002**, *43*, 303.
- Springsteen, G.; Wang, B. *Tetrahedron* **2002**, *58*, 5291.
- Yan, J.; Springsteen, G.; Deeter, S.; Wang, B. H. *Tetrahedron* **2004**, *60*, 11205.
- Caroline, C.; Sonia, A.; Chantal, L. *Polymer* **2005**, *46*, 1269.